Chemical Science

EDGE ARTICLE

View Article Online
View Journal | View Issue

Cite this: *Chem. Sci.*, 2014, **5**, 631

Towards a comprehensive understanding of platinum dissolution in acidic media

Angel A. Topalov,* Serhiy Cherevko, Aleksandar R. Zeradjanin, Josef C. Meier, Ioannis Katsounaros and Karl J. J. Mayrhofer*

Received 27th August 2013
Accepted 16th October 2013

DOI: 10.1039/c3sc52411f

www.rsc.org/chemicalscience

Platinum is one of the most important electrode materials for continuous electrochemical energy conversion due to its high activity and stability. The resistance of this scarce material towards dissolution is however limited under the harsh operational conditions that can occur in fuel cells or other energy conversion devices. In order to improve the understanding of dissolution of platinum, we therefore investigate this issue with an electrochemical flow cell system connected to an inductively coupled plasma mass spectrometer (ICP-MS) capable of online quantification of even small traces of dissolved elements in solution. The electrochemical data combined with the downstream analytics are used to evaluate the influence of various operational parameters on the dissolution processes in acidic electrolytes at room temperature. Platinum dissolution is a transient process, occurring during both positive- and negative-going sweeps over potentials of *ca.* 1.1 V_{RHE} and depending strongly on the structure and chemistry of the formed oxide. The amount of anodically dissolved platinum is thereby strongly related to the number of low-coordinated surface sites, whereas cathodic dissolution depends on the amount of oxide formed and the timescale. Thus, a tentative mechanism for Pt dissolution is suggested based on a place exchange of oxygen atoms from surface to sub-surface positions.

Introduction

Nowadays fuel cells, electrolyzers and metal–air batteries are considered as key elements in the development of sustainable energy architecture for our future societies. For several of these electrochemical energy conversion devices, platinum – typically dispersed in the form of nanoparticles on a carbon support – serves as the state of the art electrocatalyst.[1] However, the broad commercial application of such devices, for instance the application of proton exchange membrane fuel cells (PEMFCs) in the automotive industry, has not been successful so far, mainly due to the lack of stability of the electrode materials, which is one of the most important challenges still to be met. Major progress has been made in the understanding of the degradation phenomena of platinum-based electrocatalysts occurring in a fuel cell under operation, which has led to significant improvements in stability.[2–8] In particular, platinum dissolution (and eventually successive re-deposition) was demonstrated to be of tremendous importance in the course of PEMFC catalyst degradation.[1,5,9–12] Even though platinum as a noble metal is more inert towards oxidation in air than other materials, thermodynamic considerations of Pourbaix already suggest that it can be oxidized and even dissolve at potentials and pH values relevant for fuel cells.[13] Therefore, the challenge to improve platinum electrocatalyst stability for fuel cells and other electrochemical energy conversion devices demands a detailed understanding of the dissolution mechanism of platinum and the influence of the applied operational conditions. So far, high potentials,[14–16] low pH values,[17,18] transient potential conditions[19–21] and high temperatures[17,22] have been suggested as parameters that enhance platinum dissolution. Less is known on the other hand about the mechanism of platinum dissolution or the nature of the oxide species formed on the platinum surface. Some groups, for instance Rand and Woods, supported an anodic dissolution mechanism,[15,22–24] while others attributed the dissolution of platinum mainly to the electrochemical or chemical dissolution of the platinum oxide.[25–28] Despite the controversy about whether platinum dissolution predominantly occurs in the course of the positive- or negative-going scan in potential sweep experiments, most researchers agree that some form of oxide is involved in the dissolution process. Particularly interesting in this aspect are the studies of Conway and co-workers, who proposed that OH adsorption on platinum is followed by further oxidation and consequent sub-surface oxide formation above 1.1 V_{RHE},[29,30] *i.e.* a place exchange mechanism is taking place. *In situ* X-ray scattering confirmed the existence of interfacial place exchange between O_{chem} and top-layer atoms of platinum.[31] In general, however, the details of the complex chemistry of potential-dependent Pt oxidation are still largely unresolved.

Department of Interface Chemistry and Surface Engineering, Max-Planck-Institut für Eisenforschung GmbH, Max-Planck-Strasse 1, 40237 Düsseldorf, Germany. E-mail: topalov@mpie.de; mayrhofer@mpie.de; Fax: +49 211 6792 218; Tel: +49 211 67 92 160

Studies of the underlying dissolution mechanism and its potential dependence are rather challenging, mainly due to the low dissolution rate of platinum. Because of this, electrochemical experiments generally need to be accompanied by sensitive analytical methods. Our group has recently presented a technique that enables experiments with an electrochemical scanning flow cell (SFC) in combination with the time-resolved monitoring of dissolved species in the electrolyte using an inductively coupled plasma mass spectrometer (ICP-MS).[32] This unique approach combines the advantages of an electrochemical flow cell with the high accuracy of trace analysis *via* ICP-MS and was successfully utilized for *in situ* investigations of corrosion processes on several noble materials.[33–36] In this context, we also performed some first investigations on platinum in 0.1 M $HClO_4$ with cyclic voltammetry at a constant lower potential limit (0.05 V_{RHE}) and varying overpotentials for oxide formation. Platinum dissolution was observed only when the upper potential limit exceeded about 1.1 V_{RHE}, and the amount of dissolved platinum increased with increasing upper potential limit. Remarkably, when the potential was cycled from 0 to 1.3 V_{RHE} or even higher values, a clear separation of two dissolution peaks could be detected by the ICP-MS online analysis,[21] which is qualitatively in agreement with the findings of Sugawara *et al.*[37] The two peaks in the positive and negative scan of the potential cycle were denominated as "anodic" and "cathodic" dissolution, respectively, and the cathodic dissolution was demonstrated to be more dominant in the investigated conditions. In contradiction to earlier models, no steady state dissolution of platinum could be identified at room temperature within the stability window of water that was confirmed with a sequence of potentiostatic experiments.[21]

These findings motivated us to further explore the dissolution behavior of platinum, particularly the influence of the overpotential for oxide reduction on platinum dissolution in potential cycling experiments. Moreover, we analyze the impact of the timescale of the experiments as well as the concentration of protons and anions in perchloric and sulfuric acid on the dissolution process. Based on this comprehensive study we suggest a mechanism for platinum dissolution, being well aware that the exact chemistry of the Pt oxidation is not yet completely resolved.

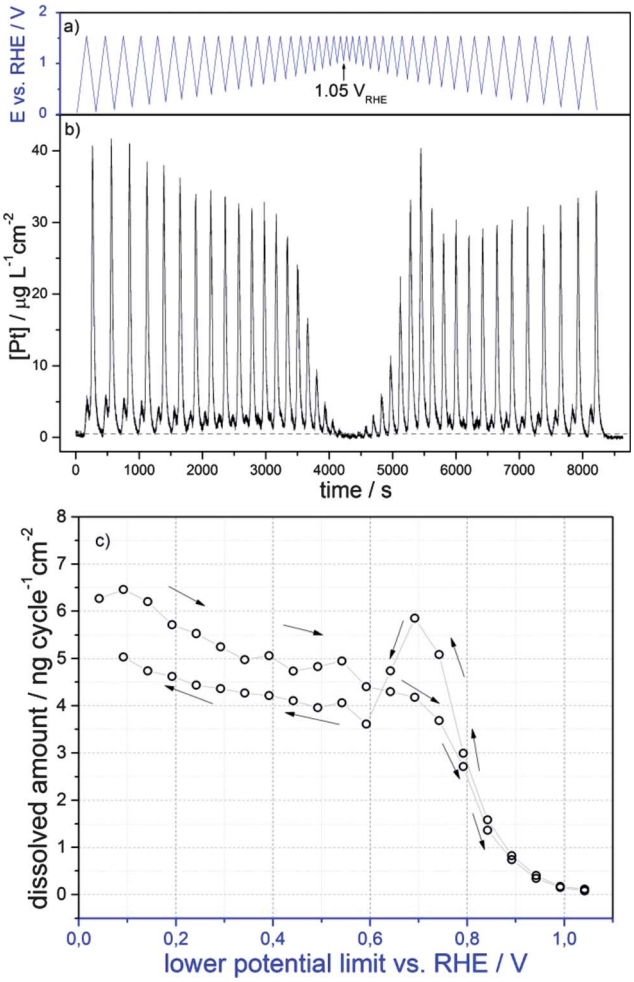

Fig. 1 (a) The applied potential sequence in 0.1 M $HClO_4$ at room temperature (cyclic voltammograms with a scan rate of 0.01 V s^{-1} and an upper potential limit of 1.55 V_{RHE}); the lower potential limit is gradually changed in steps of 0.05 V from 0.05 V_{RHE} to 1.05 V_{RHE} and down again. (b) The corresponding platinum dissolution profile plotted on the same time axis as in (a). The dashed horizontal line shows the detection limit for the measurement. (c) The integrated amount of dissolved Pt for each single cycle to different lower potential limits of the cyclic voltammograms from (b).

Results

Relation between dissolution and overpotential for Pt-oxide reduction

Platinum dissolution is strongly influenced by the applied potential and the potential transient conditions. In order to investigate dissolution processes at positive potentials with and without oxide reduction, we carried out a sequence of potential cycling experiments with a constant upper potential limit of 1.55 V_{RHE} and varying lower potential limits, complementary to the experiment described in our last report.[21] Fig. 1a depicts the applied potential cycling conditions, while Fig. 1b visualizes the amount of platinum detected online *via* ICP-MS *versus* time. Significant dissolution is present when the potential window spans over potentials that allow oxidation and reduction of the platinum surface. In contrast, as soon as the potential is not sufficiently negative to reduce platinum oxide, the dissolution rate drops. Once the potential window is narrowed to the region above the onset of platinum oxide reduction at about 1.05 V_{RHE}, dissolution almost ceases to zero. A further positive shift of the lower potential limit does not change the situation (not shown here). Due to the formation of a passive oxide layer, platinum does not dissolve significantly in the potential range where Pt-oxide is not reduced, even in transient experiments. A subsequent decrease of the lower potential limit results in the recovery of the spectrometric signal, and the integrated amount of dissolved Pt in each cycle closely follows the behavior seen when the lower potential limit was increased (Fig. 1c). The transition from an oxidized to a reduced platinum surface or *vice versa* is thus the necessary condition for significant

platinum dissolution, as seen in all our experiments at room temperature and potentials not exceeding an upper limit of 1.55 V_{RHE}. In contrast, in the potential regions (i) between 0.05 and *ca.* 1.05 V_{RHE} (ref. 21) and (ii) between *ca.* 1.05 and 1.55 V_{RHE}, potentiodynamic experiments do not result in detectable dissolution of platinum in 0.1 M $HClO_4$ at room temperature. It is a salient feature of platinum that significant dissolution only occurs when the potential is passing between these two "stability windows".

Timescale of the experiment in relation to Pt dissolution

While a strong influence of electrode potential on platinum dissolution is evident, much less is known about the impact of the potential scan rate. The observation made by Kinoshita *et al.* that triangular-wave potential cycles result in more significant platinum dissolution than square-wave potential cycles directly suggests that varying the time of potential transitions by the scan rate is important for a fundamental understanding.[38] Fig. 2a and b depict the experimental protocol with different scan rates and the signal of online detected platinum, respectively. Increasing the scan rate from 0.005 to 0.5 V s^{-1} leads to a reduction in the amount of dissolved platinum from 5.9 to 1 ng cm^{-2} $cycle^{-1}$, as summarized in Fig. 2c. A more detailed investigation of the cyclic voltammograms reveals that the amount of oxide formed on the platinum surface also depends on the scan rate. Based on the integration of the charge for Pt-oxide reduction, the oxide coverage increases with decreasing scan rate, as the system has more time to equilibrate at high potentials. Fig. 2c compares the oxide coverage determined from each negative scan with the amount of dissolved platinum from the same cycle. Assuming that the reduction of a monolayer of platinum oxide would result in a charge of 0.42 mC cm^{-2},[39] and taking into account a roughness factor of the electrode of 1.3, we can conclude that no more than about 1.5 monolayers of oxide are formed under the applied conditions, as depicted in Fig. 2c. It is important to note that the dissolution charge is about 2 orders of magnitude smaller than the charge for the surface oxide reduction. An amount of 1 ng cm^{-2} of dissolved platinum (assuming Pt^{2+} as the only dissolution product) would be equal to a charge of about 0.99 μC cm^{-2}, while the charge for the oxide reduction is in the range above 290 μC cm^{-2}.

The dissolution during potential cycling at various scan rates occurs during both the anodic and cathodic sweeps. However, for scan rates higher than 0.01 V s^{-1}, the features overlap and cannot be resolved any more in this way. To clarify how the ratio between the two processes evolves with the scan rate, additional experiments were conducted by combining stationary polarization with transient potential scans as presented in Fig. 3. Since according to our previous observation the dissolution of platinum during steady polarization is negligible at room temperature,[21] the anodic and cathodic contributions can thus also be resolved at higher scan rates. An exemplary potential profile of such a measurement and the corresponding online dissolution profile are depicted in Fig. 3a and b, respectively. The same

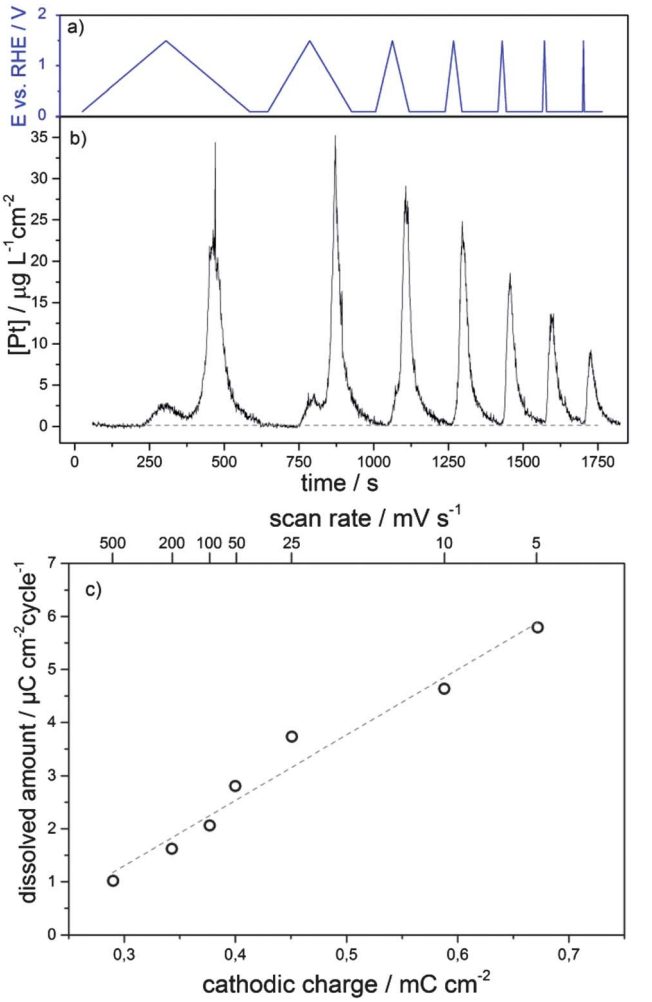

Fig. 2 (a) The applied experimental sequence in 0.1 M $HClO_4$; cyclic voltammograms between 0.05 and 1.5 V_{RHE} with scan rates of 0.005, 0.01, 0.025, 0.05, 0.1, 0.2, and 0.5 V s^{-1}. (b) The corresponding platinum dissolution profile plotted on the same time axis as in (a). The dashed line shows the detection limit for the measurement. (c) The amount of dissolved Pt for each cycle *versus* the integrated charge for Pt oxide reduction recorded during the same cycle.

experiment was conducted for six different scan rates (0.01, 0.2, 0.5, 1, 2 and 4 V s^{-1}). In addition, by changing the upper potential limit (plateaus in Fig. 3a), *i.e.* the overpotential for Pt-oxide formation, and independently determining the amount of oxide formed during one cycle, we can separate the influence of the timescale itself from the influence of the amount of formed oxide on the process of dissolution. The complete data for the dependence of platinum dissolution on the timescale of the experiment for the cathodic and anodic scans are summarized in Fig. 3c (green color) and Fig. 3d (red color), respectively.

The amount of dissolved platinum for the anodic case appears to be constant at around an average value of 0.8 ± 0.3 ng cm^{-2} (*e.g. ca.* 0.2% of a single monolayer) for all overpotentials and scan rates employed. The dissolution neither depends on the amount of oxide formed nor the time necessary to passivate the surface. It seems that the anodic dissolution

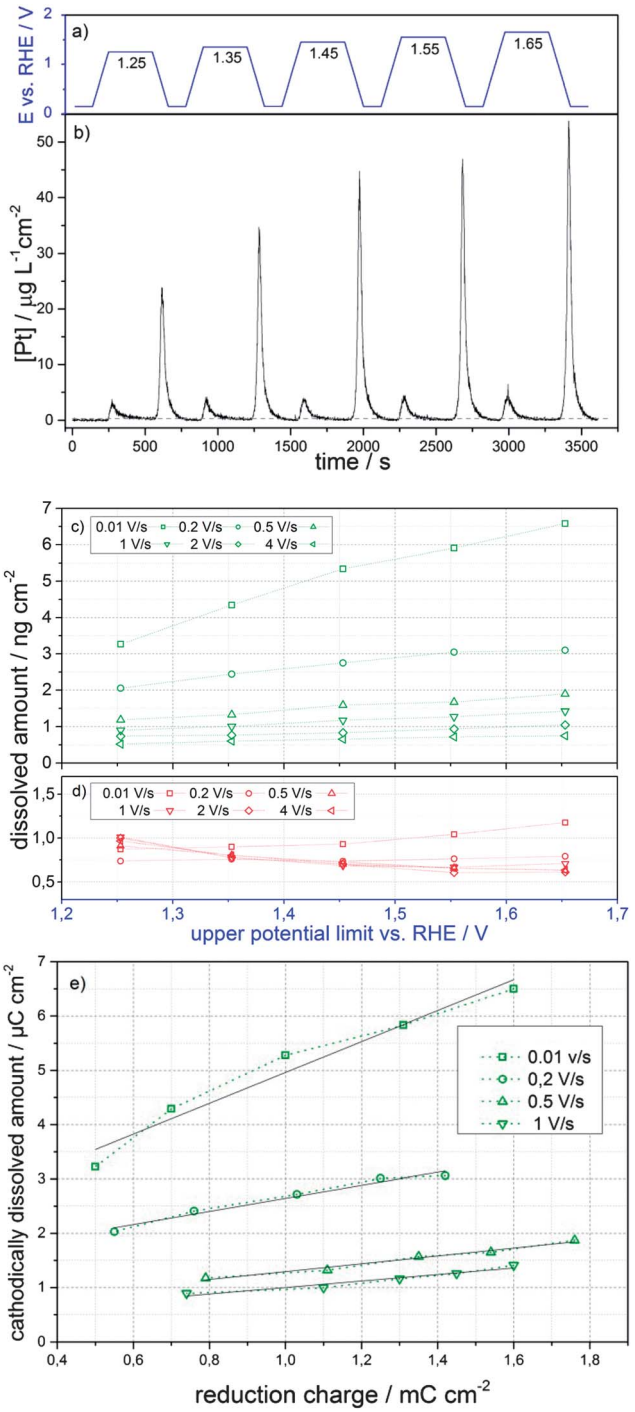

Fig. 3 (a) The applied experimental sequence in 0.1 M $HClO_4$; a potential hold at 0.05 V_{RHE} followed by a sweep with a scan rate of 0.01 V s^{-1} to the corresponding upper potential limit, hold for 300 seconds, and then a sweep back to 0.05 V_{RHE} and a successive hold. (b) The platinum dissolution profile plotted on the same time axis as in (a). The amount of dissolved platinum per sweep for the same experiments as in (a) and (b) for sweep rates of 0.01, 0.2, 0.5, 1, 2 and 4 V s^{-1} for the positive sweep in (d) and negative sweep in (c). (e) The cathodically dissolved amount plotted *versus* the reductive charge in the negative sweep.

during sub-surface oxide formation is related to the dissolution of a rather constant amount of particular platinum atoms available in the initial state.[40]

In contrast to the anodic dissolution, the cathodic counterpart is directly connected to the applied plateau potential (Fig. 3c); the higher the upper potential limit the more Pt dissolves. Moreover, while all experimental series on different timescales show qualitatively the same behavior, quantitatively they are quite different. In agreement with Fig. 2, less Pt dissolves during fast scans compared to slow ones at the same plateau potentials. This has the interesting consequence that for the same scan rate, the dissolved Pt amount scales linearly with the oxide reduction charge, but a similar reduction charge due to identical upper potentials leads to varying amounts of dissolved Pt depending on the scan rate (Fig. 3e). In other words, it is not only important how much oxide is formed, but also on what timescale it is reduced again. It is worth mentioning that the amount of dissolved platinum in the fast potential scans becomes almost independent from the amount of formed oxide and adopts values comparable to anodic dissolution.

Influence of the concentration of protons on Pt dissolution

The pH dependence of platinum dissolution has been studied by several groups, recently for instance by Tsuru and coworkers, who demonstrated that increasing the concentration of sulfuric acid enhances the rate of platinum dissolution.[18] To address this aspect we monitored platinum dissolution during potential cycling in sulfuric and perchloric acid at various concentrations and thus unavoidably changed both the pH of the solution as well as the amount of spectator species present in the electrolyte. In Fig. 4 the amount of dissolved platinum is plotted with respect to the upper potential limit of the cyclic voltammograms for perchloric and sulfuric acids.

The onset of platinum dissolution on the reversible hydrogen electrode scale coincides for all measurements around 1.1 V_{RHE}, independent of the electrolyte concentration, which suggests a proton dependent reaction is involved in the rate-determining step of platinum dissolution. The slight positive shift in the onset for sulfuric acid may be rationalized as a result of a difference in adsorption strength of the electrolyte anions, since the stronger adsorption of sulfates/bisulfates compared to perchlorates is known to result in a shift in the onset of platinum oxidation (chemisorption of OH or O).[41] Two peaks can be separated again for the positive and negative scan. The red color represents the amount of platinum dissolved in the anodic part of the cycle, which shows a minor increase with the rise of the acid concentration and the upper potential. The values are scattered around 1 ± 0.3 ng cm^{-2} $cycle^{-1}$, which suggests a moderate effect of pH on anodic dissolution for concentrations up to 1 M. An enhanced anodic dissolution was only observed in the case of 5 M $HClO_4$. The main contribution to the overall dissolution comes from the cathodic sweep, as shown in the previous experiments, and originates from the oxide reduction. The amount of cathodically dissolved platinum scales with the acidity of the electrolyte, which suggests a strong influence of the concentration of protons on the reduction of platinum oxide. The trends are the same for perchloric and sulfuric acid, however, the total amount

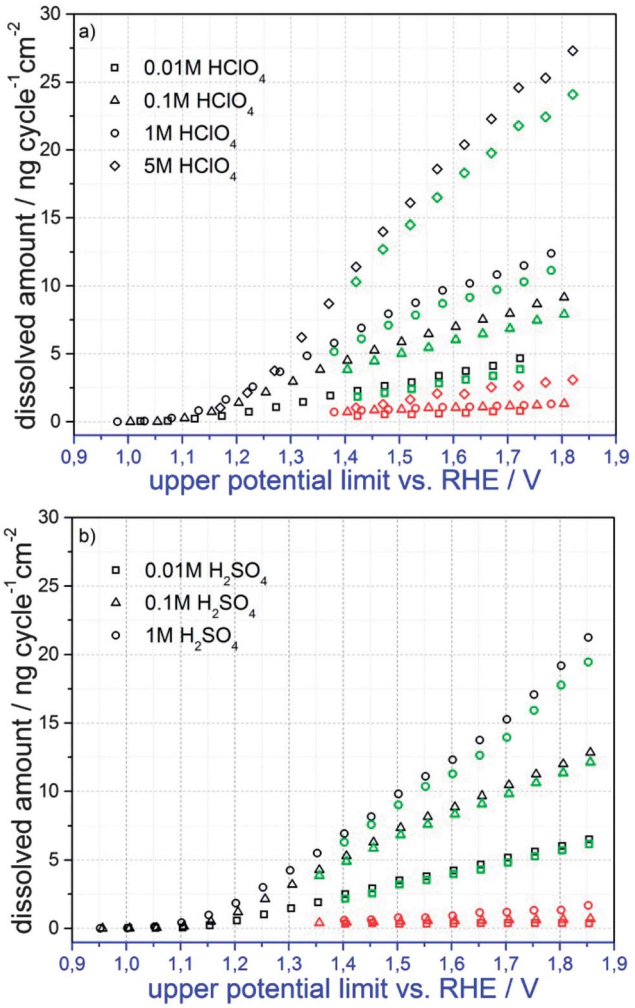

Fig. 4 The amount of dissolved platinum during potential cycling at a scan rate of 0.01 V s^{-1} between 0.05 V_{RHE} and the corresponding upper potential in (a) $HClO_4$ and (b) H_2SO_4 with different concentrations (in black). The red and green color codes show the dissolved amount during the positive and negative sweeps for the corresponding concentrations; (◇) 5 M, (○) 1 M, (Δ) 0.1 M and (□) 0.01 M.

of dissolved platinum is slightly higher in the latter one at similar concentration.

Discussion

To grasp the meaning beyond the above shown phenomenological relations, it is necessary to first summarize the most important experimental findings. Platinum dissolution is a transient process – significantly occurring only during potential change with time above a critical potential of approximately 1.1 V_{RHE}. Moreover, the dissolution can be separated into anodic and cathodic dissolution, where cathodic prevails with respect to the overall amount of dissolved Pt. While the cathodic dissolution depends strongly on the pH, anion concentration, scan rate and the potential limits, the anodic dissolution is by far less influenced by these parameters. Overall, platinum dissolution is a process that is closely related to the formation and reduction of Pt-oxides as obvious from all the experiments above. Table 1 illustrates the distinct behavior of Pt during anodic and cathodic dissolution in light of the relevant parameters.

Due to the high relevance for the dissolution process, it is worth revising some of the existing concepts for Pt oxidation; being well aware that the understanding of the true nature of the oxide is still suffering. Thermodynamically the oxidation of the Pt surface can be described by the following reactions (not considering the formation of PtO_3 at more positive potentials).

$$Pt + H_2O \leftrightarrow PtO + 2H^+ + 2e^- \quad (1a)$$

$$PtO + H_2O \leftrightarrow PtO_2 + 2H^+ + 2e^- \quad (1b)$$

During anodic polarization, an initial oxidation of the platinum surface in the region between 0.8 and 0.9 V_{RHE} is related to OH adsorption (one electron process) or direct adsorption of O^{2-} (two electron process).[29,42] Note that we refer in both cases to chemisorbed oxygenated species, independent of their true nature. Below a critical coverage of oxygenated species, the enthalpy of formation of the chemisorbed phase is higher than the enthalpy of formation of a bulk oxide. As the coverage with oxygenated species approaches the critical value, the repulsive interactions between the O adatoms gradually reduce the enthalpy of chemisorption until it becomes equal to the enthalpy of formation of the oxide. Above the critical coverage, repulsive interactions in the densely packed electronegative O adlayer induce an occupation of then energetically favorable sub-surface sites, which is usually coined as place-exchange.[43,44] In other words, the downshift of the Fermi level induced by extensive anodic polarization is first compensated by electrons provided from adsorbed oxygenated species and further by inversion of the Pt–O dipole. Based on the analysis of Conway and co-workers it can be assumed that a full coverage with OH is achieved at about 1.1 V_{RHE}.[29] Alternatively, when assuming a direct adsorption of O^{2-} (two electron process) instead of hydroxide and that O^{2-} requires two platinum sites for adsorption, full coverage would also be achieved at the same potential.[45] According to these observations place-exchange is expected to gradually start occurring at a critical coverage around or slightly below the potential of full coverage of chemisorbed oxygenated species.

Considering that the thermodynamically predicted potential for electrochemical Pt dissolution is in a similar range as the oxidation (E_0 = 1.19 V_{SHE}), it might be assumed that the equilibrium between the dissolution of reduced Pt (reaction (2)), surface passivation (reaction (1)), and chemical dissolution of the oxide (reaction (3)) is governing the electrode processes. The independence of anodic dissolution from the scan rate and both potential limits would support this assumption. However, Pt dissolution is in general a transient process that almost ceases as soon as the potential remains constant, which strongly speaks against dissolution controlled by a single reaction equilibrium.

$$Pt \leftrightarrow Pt^{2+} + 2e^- \quad (2)$$

$$PtO + 2H^+ \leftrightarrow Pt^{2+} + H_2O \quad (3)$$

Table 1 Summary of the distinct behavior of anodic and cathodic transient dissolution in acidic media

Parameters	Anodic dissolution	Cathodic dissolution
Time dependence	Transient process	Transient process
Anodic limit	Minor influence	Significant increase with more positive anodic limit
Scan rate	Minor influence	Significant increase with lowering scan rate
Cathodic limit	Minor influence	Significant increase with more negative cathodic limit
pH	Significant increase with drop in pH	Significant increase with drop in pH

Still, the transient anodic dissolution is strongly related to the surface oxidation and in particular to the oxide place-exchange. This becomes obvious from the absence of Pt dissolution in the region of adsorption of oxygenated species on the platinum surface below 1.1 V_{RHE} in the positive-going scan, and from the significant dissolution occurring only when the critical coverage is surpassed. Only in the latter case, the inversion of the Pt–O dipole by place-exchange can lead to the exposure of oxidized Pt atoms (Pt_{ex}) at the surface. At these positive potentials the majority of Pt_{ex} atoms are then passivated by adsorption of additional oxygenated species. However, some minor amounts of Pt_{ex} are not stabilized in the surface oxide and therefore chemically dissolve into the electrolyte. It is reasonable to assume that in particular, low-coordinated Pt surface sites already present in the reduced state might be more susceptible to de-stabilization and therefore dissolution. Such an initial state effect would also explain why the anodic dissolution only slightly depends on the potential limits and the scan rate, as it just depends on the number of sites available before oxidation. In contrast to a model based on reaction equilibria, this could also explain why the dissolution rate drops to values below the detection limit when constant potentials are applied.[21] Once the exposed low-coordinated Pt_{ex} sites are dissolved and no further place-exchange occurs, the remaining Pt_{ex} are stabilized in the surface oxide. Scheme 1a illustrates the transient processes during positive potential scans.

In contrast to the anodic dissolution, the dominating cathodic dissolution strongly depends on the scan rate. Moreover, it appears several hundreds of millivolts below the equilibrium potential for electrochemical dissolution (eqn (2)). Thus this transient process is even less likely to be related to reaction equilibria between dissolution, passivation and chemical dissolution. As for the anodic dissolution, Pt oxide and place-exchange play a key role in the cathodic dissolution process. The dissolution occurs in parallel with the reduction of the surface below 1.05 V_{RHE} after potential excursions above 1.1 V_{RHE}, and the amount of dissolved Pt scales with the applied potential, *i.e.* with the amount of oxidized, but passivated Pt_{ex} atoms in the initial state before a negative-going scan. During the reduction of the surface, these sites become exposed to the electrolyte and can then potentially be dissolved. Due to the large amount of formed place-exchanged atoms at high potentials, the cathodic dissolution rate is generally higher than the anodic one. However the dissolution charge is two orders of magnitude lower than the charge required for oxide reduction. The reason for the latter is the competition of dissolution with either deposition of mobile Pt_{ex} species or re-deposition of dissolved Pt on already reduced Pt sites available at the low potentials during reduction. An enhanced scan rate would favor the kinetics for (re-)deposition and thus lead to less dissolution as observed, while an increased acidity promotes the chemical dissolution of Pt_{ex}. The possible pathways for the cathodic dissolution are illustrated in Scheme 1b.

In summary, both anodic and cathodic dissolution are initiated by the electrochemical oxidation/reduction of the Pt surface, in particular the place-exchange between Pt–O, followed by a chemical dissolution of the transiently exposed Pt_{ex} sites. The differences between the processes are the initial state before the formation of the oxide and before the reduction of the oxide, and the competing reactions of passivation and (re-)deposition, respectively.

Conclusions

In this work we have presented a detailed investigation of the dissolution behavior of polycrystalline platinum in acid electrolyte under various experimental conditions. Utilizing an advanced experimental approach based on online mass spectrometry, the dissolution profiles during electrochemical treatment were monitored in parallel to the current response. Thus,

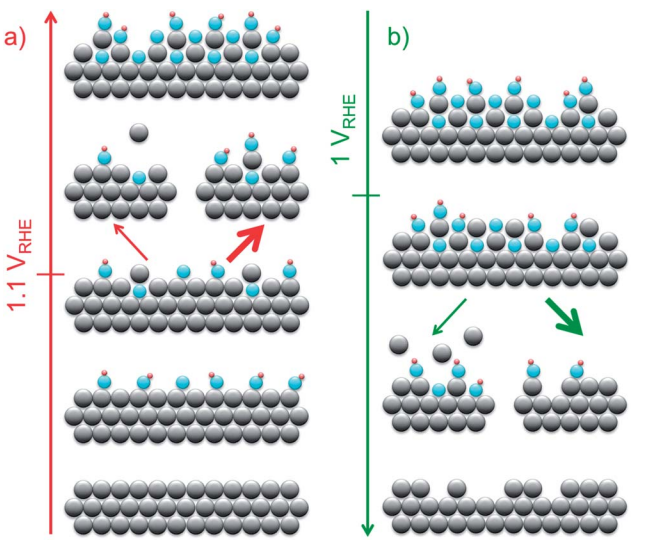

Scheme 1 Alternation of the platinum surface state during: (a) anodic polarization, above *ca.* 1.1 V_{RHE} dissolution and passivation of the surface are in competition; and (b) cathodic polarization, during surface reduction below *ca.* 1.0 V_{RHE} (re-)deposition and dissolution are in competition.

a straightforward separation of the anodic and cathodic dissolution processes was presented in correlation with the formation and reduction of the oxide layer. The anodic dissolution was only slightly dependent on the chosen potential limits in cyclic voltammetry, the scan rate, and the pH of the electrolyte, while clearly an enhanced cathodic dissolution was observed with higher anodic potential limits, lower scan rates and increased acidity. Based on these observations on platinum in acidic media a dissolution mechanism for both the anodic and the cathodic path is proposed. According to this mechanism, Pt dissolution is a transient process initiated by the formation and reduction of sub-surface oxygen and strongly depends on the initial state of the surface.

Experimental part

A polycrystalline platinum foil purchased from MaTeck (purity 99.99%) is used as a working electrode. The surface of the foil was ground and polished with a 1 μm diamond suspension. To serve as the working electrode, the sample was fixed on a three dimensional translational stage and contacted with a tungsten needle. Before each measurement, the surface was electrochemically cleaned by 50 potential cycles between 0.05 and 1.5 V_{RHE} at a scan rate 0.2 V s^{-1}. The roughness factor, estimated from H_{UPD}, was about 1.3 in all measurements. In the current work all values were normalized to the geometric area contacted with the cell, *i.e.* 1.1 mm^2. The experiments were performed using a home-made micro-electrochemical scanning flow cell (SFC) directly coupled to an inductively coupled plasma mass spectrometer (ICP-MS). The cell is based on the concept of a channel electrode with V-formed geometry made of polyacrylate.[46] All hardware components were controlled *via* an in-house made LabVIEW software.[47] A constant electrolyte flow was sustained through the channels by the MP^2 peristaltic pump of the ICP-MS (NexION 300X, Perkin Elmer) situated downstream of the electrochemical cell. The dissolution profiles were monitored over two isotopes ^{193}Pt and ^{195}Pt with respect to 7.5 μg L^{-1} ^{187}Re as internal standard. The spectrometric data was recorded with 50 ms dwell time and 5 sweeps per reading over the three isotopes, which results in an acquisition rate of 1 Hz. At a potential scan rate of 10 mV s^{-1} this corresponds to an uncertainty of *ca.* ±10 mV in the onset potential. The delay time between electrode dissolution and spectrometric detection was *ca.* 15–20 s, which was corrected for by separate pulse experiments. The peak broadening due to convection in the thin pipes to the ICP-MS inlet was not corrected for. The mixing with the internal standard was performed directly after the SFC. A performance check and calibration of the ICP-MS was carried out on each experiment day. The system is discussed in more detail in our previous reports.[32,36] The electrolytes were freshly prepared from suprapure $HClO_4$ and H_2SO_4 (Merck) and diluted in ultrapure water (ELGA, 18.2 MΩ) to obtain the required concentrations of 0.01, 0.1, 1 and 5 mol L^{-1}. All electrolytes were continuously deaerated with argon (purity 5.0) before and during the measurements. All experiments were performed at room temperature (*ca.* 295 K).

Acknowledgements

We thank the BMBF (Kz: 033RC1101A) for financial support. J.C.M. acknowledges financial support by the Kekulé Fellowship from the Fond der Chemischen Industrie (FCI). We acknowledge Andrea Mingers for experimental assistance.

Notes and references

1 *Handbook of fuel cells: fundamentals, technology, and applications*, ed. W. Vielstich, A. Lamm and H. A. Gasteiger, Wiley, Chichester, England; Hoboken, N.J., 2003.
2 R. Borup, J. Meyers, B. Pivovar, Y. S. Kim, R. Mukundan, N. Garland, D. Myers, M. Wilson, F. Garzon, D. Wood, P. Zelenay, K. More, K. Stroh, T. Zawodzinski, J. Boncella, J. E. McGrath, M. Inaba, K. Miyatake, M. Hori, K. Ota, Z. Ogumi, S. Miyata, A. Nishikata, Z. Siroma, Y. Uchimoto, K. Yasuda, K. Kimijima and N. Iwashita, *Chem. Rev.*, 2007, **107**, 3904–3951.
3 *Polymer electrolyte fuel cell degradation*, ed. M. Mench, E. C. Kumbur and T. N. Veziroglu, Academic Press, Amsterdam, Boston, 2012.
4 S. Zhang, X. Yuan, H. Wang, W. Merida, H. Zhu, J. Shen, S. Wu and J. Zhang, *Int. J. Hydrogen Energy*, 2009, **34**, 388–404.
5 Y. Shao-Horn, W. C. Sheng, S. Chen, P. J. Ferreira, E. F. Holby and D. Morgan, *Top. Catal.*, 2007, **46**, 285–305.
6 K. Schlögl, M. Hanzlik and M. Arenz, *J. Electrochem. Soc.*, 2012, **159**, B677.
7 J. C. Meier, C. Galeano, I. Katsounaros, A. A. Topalov, A. Kostka, F. Schüth and K. J. J. Mayrhofer, *ACS Catal.*, 2012, **2**, 832–843.
8 J. C. Meier, I. Katsounaros, C. Galeano, H. Bongard, A. A. Topalov, A. Kostka, A. Karschin, F. Schuth and K. J. J. Mayrhofer, *Energy Environ. Sci.*, 2012, **5**, 9319–9330.
9 J. Aragane, *J. Electrochem. Soc.*, 1988, **135**, 844.
10 F. J. Perez-Alonso, C. F. Elkjær, S. S. Shim, B. L. Abrams, I. E. L. Stephens and I. Chorkendorff, *J. Power Sources*, 2011, **196**, 6085–6091.
11 C. Galeano, J. C. Meier, V. Peinecke, H. Bongard, I. Katsounaros, A. A. Topalov, A. Lu, K. J. J. Mayrhofer and F. Schüth, *J. Am. Chem. Soc.*, 2012, **134**, 20457–20465.
12 N. Hodnik, M. Zorko, B. Jozinović, M. Bele, G. Dražič, S. Hočevar and M. Gaberšček, *Electrochem. Commun.*, 2013, **30**, 75–78.
13 M. Pourbaix, *Atlas of electrochemical equilibria in aqueous solutions*, Nat'L Assoc. of Corrosion, [S.l.], 1974.
14 A. N. Chemodanov, Y. M. Kolotyrkin and M. A. Dembrovski, *Elektrohimia*, 1970, **6**, 460–468.
15 A. Damjanovic, A. Dey and J. O. Bockris, *J. Electrochem. Soc.*, 1966, **113**, 739.
16 Y. M. Kolotyrkin, V. V. Losev and A. N. Chemodanov, *Mater. Chem. Phys.*, 1988, **19**, 1–95.
17 S. Mitsushima, Y. Koizumi, S. Uzuka and K.-I. Ota, *Electrochim. Acta*, 2008, **54**, 455–460.
18 A. P. Yadav, T. Okayasu, Y. Sugawara, A. Nishikata and T. Tsuru, *J. Electrochem. Soc.*, 2012, **159**, C190.

19 S. Mitsushima, S. Kawahara, K. Ota and N. Kamiya, *J. Electrochem. Soc.*, 2007, **154**, B153.
20 R. M. Darling and J. P. Meyers, *J. Electrochem. Soc.*, 2003, **150**, A1523.
21 A. A. Topalov, I. Katsounaros, M. Auinger, S. Cherevko, J. C. Meier, S. O. Klemm and K. J. J. Mayrhofer, *Angew. Chem., Int. Ed.*, 2012, **51**, 12613–12615.
22 G. Inzelt, B. Berkes and Á. Kriston, *Electrochim. Acta*, 2010, **55**, 4742–4749.
23 D. A. J. Rand and R. Woods, *J. Electroanal. Chem. Interfacial Electrochem.*, 1972, **35**, 209–218.
24 A. P. Yadav, A. Nishikata and T. Tsuru, *J. Electrochem. Soc.*, 2009, **156**, C253.
25 D. C. Johnson, D. T. Napp and S. Bruckenstein, *Electrochim. Acta*, 1970, **15**, 1493–1509.
26 F.-B. Li, A. Robert Hillman, S. D. Lubetkin and D. J. Roberts, *J. Electroanal. Chem.*, 1992, **335**, 345–362.
27 S. Kawahara, S. Mitsushima, K. Ota and N. Kamiya, *ECS Trans.*, 2006, **3**, 625–631.
28 M. Umeda, Y. Kuwahara, A. Nakazawa and M. Inoue, *J. Phys. Chem. C*, 2009, **113**, 15707–15713.
29 H. Angerstein-Kozlowska, B. E. Conway and W. B. A. Sharp, *J. Electroanal. Chem. Interfacial Electrochem.*, 1973, **43**, 9–36.
30 B. V. Tilak, B. E. Conway and H. Angerstein-Kozlowska, *J. Electroanal. Chem. Interfacial Electrochem.*, 1973, **48**, 1–23.
31 Z. Nagy and H. You, *Electrochim. Acta*, 2002, **47**, 3037–3055.
32 S. O. Klemm, A. A. Topalov, C. A. Laska and K. J. J. Mayrhofer, *Electrochem. Commun.*, 2011, **13**, 1533–1535.
33 S. Cherevko, A. A. Topalov, I. Katsounaros and K. J. J. Mayrhofer, *Electrochem. Commun.*, 2013, **28**, 44–46.
34 G. N. Ankah, A. Pareek, S. Cherevko, A. A. Topalov, M. Rohwerder and F. U. Renner, *Electrochim. Acta*, 2012, **85**, 384–392.
35 A. K. Schuppert, A. A. Topalov, A. Savan, A. Ludwig and K. J. J. Mayrhofer, *ChemElectroChem*, 2013, DOI: 10.1002/celc.201300078.
36 S. O. Klemm, A. Karschin, A. K. Schuppert, A. A. Topalov, A. M. Mingers, I. Katsounaros and K. J. J. Mayrhofer, *J. Electroanal. Chem.*, 2012, **677–680**, 50–55.
37 Y. Sugawara, T. Okayasu, A. P. Yadav, A. Nishikata and T. Tsuru, *J. Electrochem. Soc.*, 2012, **159**, F779–F786.
38 K. Kinoshita, J. T. Lundquist and P. Stonehart, *J. Electroanal. Chem. Interfacial Electrochem.*, 1973, **48**, 157–166.
39 V. A. T. Dam and F. A. de Bruijn, *J. Electrochem. Soc.*, 2007, **154**, B494.
40 Y. Onochi, M. Nakamura and N. Hoshi, *J. Phys. Chem. C*, 2012, **116**, 15134–15140.
41 B. E. Conway, *Prog. Surf. Sci.*, 1995, **49**, 331–452.
42 G. Jerkiewicz, G. Vatankhah, J. Lessard, M. P. Soriaga and Y.-S. Park, *Electrochim. Acta*, 2004, **49**, 1451–1459.
43 C. Parkinson, M. Walker and C. McConville, *Surf. Sci.*, 2003, **545**, 19–33.
44 D. L. Bashlakov, L. B. F. Juurlink, M. T. M. Koper and A. I. Yanson, *Catal. Lett.*, 2011, **142**, 1–6.
45 M. L. B. Rao, A. Damjanovic and J. O. Bockris, *J. Phys. Chem.*, 1963, **67**, 2508–2509.
46 A. K. Schuppert, A. A. Topalov, I. Katsounaros, S. O. Klemm and K. J. J. Mayrhofer, *J. Electrochem. Soc.*, 2012, **159**, F670–F675.
47 A. A. Topalov, I. Katsounaros, J. C. Meier, S. O. Klemm and K. J. J. Mayrhofer, *Rev. Sci. Instrum.*, 2011, **82**, 114103.